Evaluation of High-Resolution Ocean Surface Vector Winds Measured by QuikSCAT Scatterometer in Coastal Regions

Wenqing Tang, W. Timothy Liu, and Bryan W. Stiles

***Abstract*—The SeaWinds scatterometer onboard QuikSCAT covers approximately 90% of the global ocean under clear and cloudy condition in 24 h, and the standard data product has 25-km spatial resolution. Such spatial resolution is not sufficient to resolve small-scale processes, especially in coastal oceans. Based on range-compressed normalized backscatter and a modified wind retrieval algorithm, a coastal wind dataset at 12.5-km resolution was produced. Even with larger error, the high-resolution winds, in medium to high strength, would still be useful over coastal ocean. Using measurements from moored buoys from the National Buoy Data Center, the high-resolution QuikSCAT wind data are found to have similar accuracy as standard data in the open ocean. The accuracy of both high- and standard-resolution winds, particularly in wind directions, is found to degrade near shore. The increase in error is likely caused by the inadequacy of the geophysical model function/ambiguity removal scheme in addressing coastal conditions and light winds situations. The modified algorithm helps to bring the directional accuracy of the high-resolution winds to the accuracy of the standard-resolution winds in near-shore regions, particularly in the nadir and far zones across the satellite track.**

***Index Terms*—Coastal ocean, scatterometer, vector wind.**

I. Introduction

THE SeaWinds scatterometer onboard of the National Aeronautics and Space Administration (NASA) QuikSCAT satellite has been successfully collecting data since July 1999. The SeaWinds radar system sends microwave pulses to, and measures the power backscattered from, the earth's surface. The backscatter is largely determined by the roughness of the surface, which is, over the ocean, due to the small centimeter-scale waves. The idea of remote sensing of ocean surface winds was based on the belief that these ripples are in equilibrium with the local wind stress. The backscatter depends not only on the magnitude of the wind stress but also the wind direction relative to the direction of the radar beam (azimuth angle). The capability of measuring both wind speed and direction is the major characteristic of the scatterometer. The quality of the scatterometer vector wind fields has been rigorously validated [1]–[3] and applied to various scientific applications [4].

The QuikSCAT standard wind product [5], with 25-km resolution, is derived from normalized backscattered power σ_o returned from an ellipsoidal instantaneous antenna footprint (so-called "egg"). The 25-km spatial resolution is not sufficient for studying many interesting oceanic processes, such as storms, fronts, and coastal upwelling. The radar signal-processing system on SeaWinds/QuikSCAT has implemented the technique of range compression of a backscattered signal [6]. Using onboard filtering, the "egg" can be divided into smaller, contiguous "slices." The computation of backscatter and wind from "slices" will, in principle, provide higher spatial resolution. Case studies have demonstrated that high-resolution vector wind retrieved from "slices" reveals new features in Hurricane Floyd [7], Catalina Eddy [8], and Santa Ana Winds [9]. Because "slices" are expected to be noisier than "eggs," our first objective of this study is to assess any degradation in the wind fields introduced by using "slices" instead of "eggs."

Spatial resolution is particularly important to resolve the high variability of coastal winds under the influence of land. In the standard QuikSCAT data processing, σ_o measurements with any part of its footprint touching land were excluded in the wind retrieval. This results in a data gap within 25 km from the shoreline. Although this very stringent criterion ensures that the retrieved wind will be completely free from land contamination, it also excludes large amounts of data in areas crucial to coastal study. Our second objective is to explore how to relax the land contamination criteria and preserve some useful wind measurements in the 25-km zone from the shoreline.

Many efforts have been devoted to producing high-resolution QuikSCAT vector wind fields. Long *et al.* [10] demonstrated the ability to retrieve ultra-high-resolution wind based on scatterometer backscatter estimates created by applying image reconstruction/resolution enhancement technique. Chao *et al.* [11] created high-resolution wind for coastal oceans by combining scatterometer measurements with a regional mesoscale model. The QuikSCAT project produces wind at 12.5-km resolution in near-real time for operational forecast, using a similar approach as this study based on "slice," with a simplified backscatter averaging scheme and different land contamination criteria.

In this study, the standard wind retrieval process was modified to retrieve vector wind at 12.5-km resolution from "slices" under relaxed land contamination criteria. We processed data

Manuscript received September 26, 2003; revised March 30, 2004. The work described in this paper was carried out at the Jet Propulsion Laboratory, California Institute of Technology, under contract with the National Aeronautics and Space Administration (NASA) and was supported in part by the National Oceanic and Atmospheric Administration Office of Global Programs.

The authors are with the Jet Propulsion Laboratory, Pasadena, CA 91109 USA (e-mail: Wenqing.Tang@jpl.nasa.gov).

Digital Object Identifier 10.1109/TGRS.2004.831685

U.S. Government work not protected by U.S. copyright.

in the domain along the west coast of North America, from May to October 2002. Details on how the high-resolution wind data was produced will be described in Section II. The product was evaluated using measurements from National Buoy Data Center (NDBC) moored buoys, and compared with the standard QuikSCAT product. Realizing the fundamental difference between scatterometer (spatial average of instantaneous measurements) and buoy (temporal means of measurements at a fixed point) [2], [12], the evaluation was conducted from several perspectives, as presented in Section III.

II. High-Resolution QuikSCAT Data

The data algorithm for SeaWinds is originally designed for the NASA Scatterometer (NSCAT). In the standard data product, the spatial resolution of the σ_o measurements is determined by the dimensions of the antenna beam footprint on the earth surface, i.e., "beamlimited." The conically scanning dual "pencil-beam" system produces an egg-shaped footprint on the earth's surface of dimensions about 25 km $\times$ 35 km. All the independent "looks" returned from the footprint were used to compose a single "egg" σ_o measurement. "Eggs" were then grouped into wind vector cells (WVCs) on regular grid at 25-km resolution along and across the satellite track in terms of the location of the footprint centroid. Wind speed and direction are retrieved from σ_o measurements through a geophysical model function (GFM). Variance of the σ_o measurement, which related to the number of "looks" available in the footprint, directly affects the performance of wind retrieval algorithm. The spatial resolution of the QuikSCAT standard level 2B ocean vector wind (commonly called L2B, will be referred to as LR in this paper) is determined by the smaller dimension (25 km) of the footprint.

With the range compression filtering implemented on SeaWinds/QuikSCAT, each "egg" is resolved into several "slices" [6]. Instead of the whole footprint, all the "looks" within each slice now are used to compose a "slice" σ_o measurement. If each footprint is divided into five slices, the effective spatial dimension becomes 25 km $\times$ 7 km. Portabella and Stoffelen [13] compared two sets of QuikSCAT data (both at 25-km resolution) based on "egg" and "slice," respectively, and found that although their maxima of a likelihood estimate (MLE) distributions were very different, the quality of retrieved winds was similar. When "slices" are used for high-resolution wind retrieval, it is expected that the 12.5-km wind fields have more intrinsic noise than the standard products, due to fewer measurements used. The question is to what degree such degradation is tolerable.

Based on "slices," we produced high-resolution wind data (HR) using basically the same algorithm of LR. "Slices" are grouped into WVCs, depending on the center location of the "slice," on a finer grid (12.5 km) along and cross the satellite track. For low-resolution data, the land contamination criterion was to screen out any footprint that "touches" land [5]. This was relaxed in the high-resolution wind processing to include "slices" whose centers are over the water. Up to four ambiguous wind vector solutions are produced through GMF corresponding to the local MLE. However, the relative likelihood estimates alone are not sufficient to choose the unique wind solution, due to inaccuracies in measurement and model function. Information from surrounding WVCs are then incorporated in the ambiguity removal process based on assumption that an individual wind vector should fit in the geophysical wind pattern in the surrounding local area. A spatial median filter is applied iteratively to select a single wind vector from the ambiguities that is closest to the median of the surrounding 7 $\times$ 7 WVCs. It is noted that when the median filtering process approaching the shoreline, only part of the filtering area is filled with available data.

For QuikSCAT, the rate at which the likelihood value drops off from the maxima varies with cross-track distance. There are zones in the data swath where the likelihood estimates are very similar over a large range of wind direction. The direction interval retrieval (DIR) algorithm [14] was developed to address this problem. Instead of selecting wind vectors from a set of discrete solution set corresponding to local MLEs, DIR finds the wind direction along a one-dimensional segment of a best speed ridge around the local MLEs to the best fit in the wind pattern in the area. QuikSCAT wind data at low/high resolution with DIR modification will be referred as LRD and HRD, respectively.

Scatterometer measured winds were collocated with NDBC buoy measurements to produces a database for evaluation. The hourly buoy vector winds are based on an 8-min average, with RMS error of 1.0 m/s and 10° [15], [16]. We identified 23 buoy stations, as shown in Fig. 1. Among them, 18 buoys are near shore, with the distance from the shoreline ranging from 14–80 km, and the other five stations are more than 400 km away from the land, considered representing offshore or open ocean conditions. Buoy wind speeds measured by anemometers at various heights were converted to equivalent neutral wind [17] at 10 m. Collocation criteria are within 25-km distance from buoy locations and within 30 min. The database consists of around 22 000 HR-NDBC pairs near shore, 16 000 pairs offshore; and 8500 LR-NDBC pairs near-shore, 4500 pairs offshore.

III. Evaluation Results

A. Vector Wind Accuracy

Our first effort is to assess quantitatively any degradation of HR from LR through comparison with buoy measurements. Results presented in this section are based on scatterometer winds selected by the ambiguity removal algorithm [5], not the one closest to buoys. As stated in Section II, HR was expected to be less accurate than LR, due to noisier backscatter used in wind retrieval. Table I summarizes the statistics of comparisons between LR, HR, and buoy data. Generally speaking, the quality of HR is similar as LR, in the sense that both perform much better in open ocean than near shore. Offshore, the bias and RMS difference (RMSD) for (LR-buoy) are 0.2, 0.95 m/s in speed, and 4.83°, 17.41° in direction. The corresponding values for the HR-buoy are 0.42, 1.14 m/s in speed, and 3.98°, 22.83° in direction. Although not as good as LR, the accuracy of HR

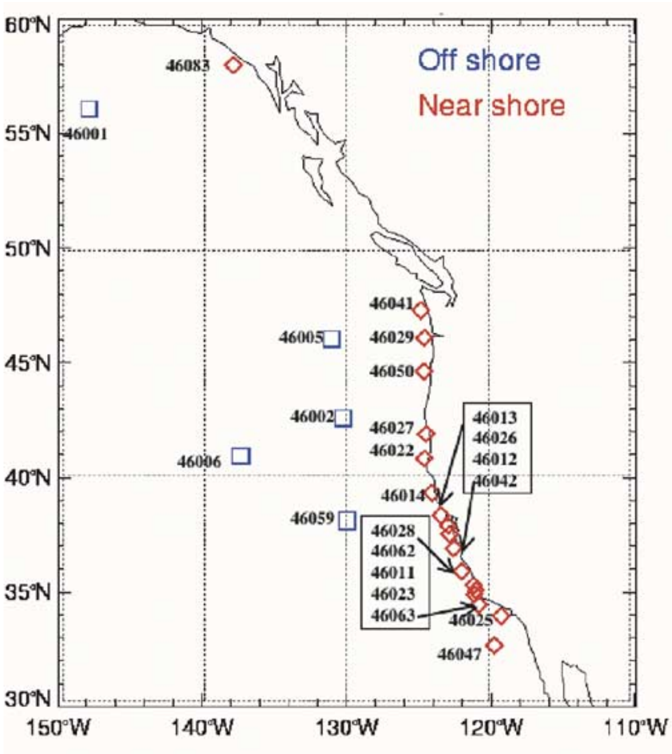

Fig. 1. Location of 23 NDBC buoys used in evaluation, among them five buoys representing open ocean conditions (blue square symbols), and 18 along the west coast of North America representing near-shore conditions (red diamond symbols).

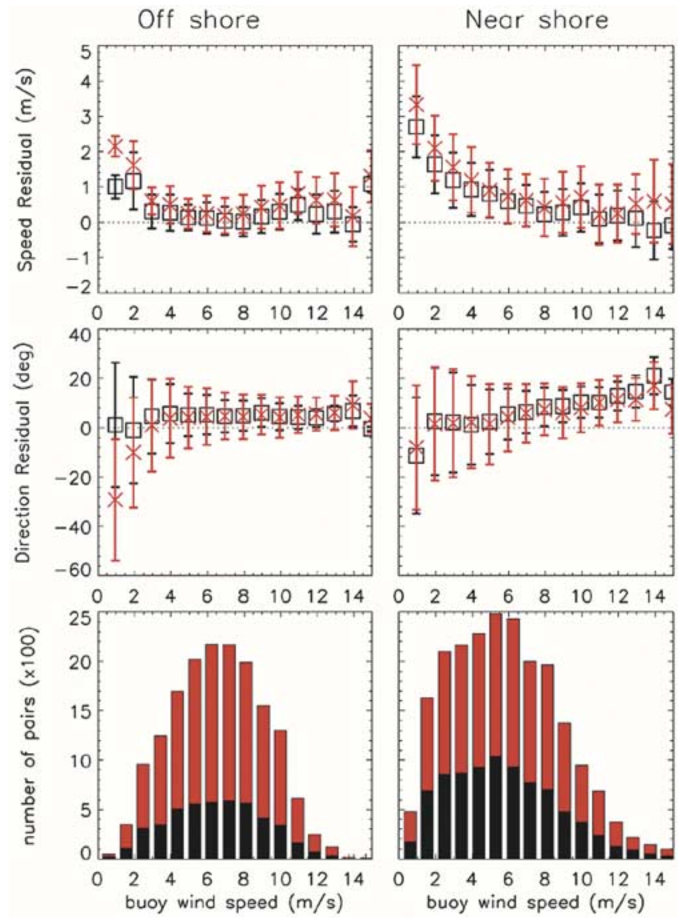

Fig. 2. (Top) Dependence of wind speed and (middle) direction residuals (scat-buoy) on the buoy wind speed at (left) offshore and (right) near-shore locations, respectively. In bins of buoy wind speed of 1 m/s, the upper two panels show (symbols) the mean and (vertical lines) standard deviation, and the low panel shows the number of pairs for QuikSCAT data LR (black) and HR (red).

satisfies or was close to the instrument specification of 2 m/s and 20°. Fig. 2 shows the residuals (scat—buoy) dependence on buoy wind speed. Data was binned into 1-m/s bins of buoy wind speed. The functional forms for HR are very similar to those of LR in both speed and direction, except in the light wind range ($<=$ 3 m/s), where HR presents much large residuals. In the medium to high wind strength, the residuals of HR and LR converge, and RMSD in direction decreasing in both HR and LR.

Performance near shore is obviously worse than offshore. However, problems exist for both LR and HR near shore. Actually, statistics show that HR is not significantly worse than LR at near shore. For LR, the bias and RMSD are increased to 0.70 and 1.50 m/s in speed, 5.5° and 26.9° in direction, corresponding to values in HR of 0.93, 1.83 m/s in speed, and 4.71°, 31.15° in direction. Although speed accuracy could still satisfy specification, the direction retrieved for both LR and HR could not. This indicates the difficulty in remotely measuring the vector wind in coastal regions, where ocean–atmosphere interactions are modified by land.

In an attempt to assess the impact of relaxing the land contamination criteria, the statistical analysis was repeated on HR by excluding data within 25 km from the shoreline, which is around 15% of the total records in the near-shore database. The statistical results were included in Table I. The residual dependence on wind speed (not shown) was between the two curves in Fig. 2, closer to HR curve at low speed. The bias and RMSD are 0.77 and 1.62 m/s in speed, and 5.41°, 29.88° in direction, with negligible difference from those with coastal zone data included (HR). This implies that the change we made in land contamination criteria does not introduce a large error in the simple statistical comparison. However, it is clear from Fig. 2 that light wind does contribute a lot to the residual. Statistical results from excluding records of buoy wind speed less than 3 and 6 m/s were also listed in Table I. The wind RMSDs, especially in wind direction, from both LR and HR were much closer to the buoy estimates after removing light wind.

Fig. 3 depicts the scat-buoy residuals at each buoy station. Contribution from individual buoy to the overall performance must be different as indicated by the large range of number of match-up pairs. However, there are common features worth pointing out. First, scatterometer wind speeds, for both LR and HR, are biased high at all locations, with HR a little higher, espatially near shore. Second, directions are clockwisely biased at most locations except station 46022. Third, the largest residuals observed at station 46027, which is closest to the land where the number of data is much less than other stations. After removing HR data falling within 25 km from the shoreline, the residuals fit right in between LR and HR (not shown).

TABLE I
STATISTICAL COMPARISON BETWEEN QSCAT DATA (LR, HR) AND NDBC BUOY WIND MEASUREMENT

	Off Shore Buoy Locations				Near Shore Buoy Locations			
	Number of data	Bias (Scat-buoy)	RMSE (Scat-buoy)	Correlation Coefficient	Number of data	Bias (Scat-buoy)	RMSE (Scat-buoy)	Correlation Coefficient
LR								
Speed (m/s)								
Buoy wind speed								
>= 0 m/s	4613	0.20	0.95	0.94	8358	0.70	1.50	0.88
>= 3 m/s	4169	0.17	0.91	0.94	6664	0.48	1.37	0.87
>= 6 m/s	2759	0.17	0.93	0.90	3826	0.27	1.33	0.84
Direction (deg.)								
Buoy wind speed								
>= 0 m/s	4613	4.83	17.41	0.98	8385	5.51	26.86	0.89
>= 3 m/s	4169	5.03	14.31	0.99	6664	6.70	20.77	0.92
>= 6 m/s	2759	4.87	11.42	0.99	3826	9.33	14.78	0.94
HR								
Speed (m/s)								
Buoy wind speed								
>= 0 m/s	16520	0.42	1.14	0.92	21415	0.93	1.83	0.84
>= 3 m/s	15162	0.37	1.14	0.91	17201	0.68	1.70	0.83
>= 6 m/s	10201	0.40	1.20	0.85	10270	0.51	1.71	0.77
Direction (deg.)								
Buoy wind speed								
>= 0 m/s	16520	3.98	22.83	0.96	21415	4.71	31.15	0.85
>= 3 m/s	15162	4.61	20.39	0.97	17201	5.73	26.37	0.87
>= 6 m/s	10201	4.84	16.90	0.98	10270	7.82	21.07	0.88
HR (off25km)								
Speed (m/s)								
Buoy wind speed								
>= 0 m/s					17763	0.77	1.62	0.87
>= 3 m/s					14459	0.58	1.57	0.85
>= 6 m/s					8654	0.45	1.62	0.79
Direction (deg.)								
Buoy wind speed								
>= 0 m/s					17763	5.41	29.88	0.86
>= 3 m/s					14459	6.47	25.04	0.88
>= 6 m/s					8654	8.56	19.62	0.90

In summary, the statistical analysis indicates that the high-resolution (12.5 km) wind retrieved from "slice" satisfies the accuracy specification for scatterometer vector winds in the open ocean. This provides a justification to reprocess almost four years of QuikSCAT data that already exists to produce high-resolution vector wind fields over global oceans. Statistics also reveal that the wind retrieval algorithm based on GMF developed empirically using data in open ocean presents larger error in coastal oceans, especially in direction, for both standard and high-resolution data products. Light winds contribute to large directional error in both open and coastal oceans. Encouragingly, relaxation of the land contamination criteria does not introduce very large residuals. However, due to a small fraction affected by land, this analysis is not meant to be complete. An appropriate flag must be included for the wind estimation obtained such way, to alert for extra caution in using the potentially useful information in the critical region.

B. Ambiguity Removal Skill

The large residual between scatterometer and buoy measurements near shore, especially in wind direction, calls for a closer examination of the ambiguity removal skill. Among up to four ambiguous solutions, the one selected is not necessarily the one closest to the buoy measurement. To further identify areas that need more improvement, the collocated database was divided in terms of the number of ambiguity. The ambiguity removal skill shown in Fig. 4 is defined as the percentage of cases where the ambiguity removal algorithm picks the wind solution closest to the buoy measurements among the total number of collocated pairs, as a function of cross-track distance. Integrated cross track, the HR ambiguity removal skills, at offshore locations, are 95.7%, 88.8%, and 89.8% for 2-, 3-, and 4-ambiguous solutions respectively. Integration over the ambiguity removal skill for LR gives 97.7%, 94.7%, and 92.9% for 2-, 3-, and 4-ambiguities. The skill degradation caused by applying the algorithm to high-resolution wind retrieval in the open ocean is about 2% to 6%, which is considered acceptable. The lowest skill is seen around nadir when 4-ambiguous solutions provided.

At near-shore buoy locations, the distributions of scatterometer solution for 2-, 3- and 4- ambiguity cases are quite similar to offshore, while the number of cases the algorithm failed to pick the best solution increases. The integrated ambiguity removal skills across track are 85.2%, 75.5%, and 76.8% for 2-, 3-, and 4-ambiguities for HR, comparing with the corresponding values for LR of 87.6%, 80.7%, and 79.5%. This loss in skill is found at the same order assessed in the similar analysis by excluding data in the 25-km coastal zone. The corresponding ambiguity removal skills, in the near-shore location, are 87.7%, 76.5%, and

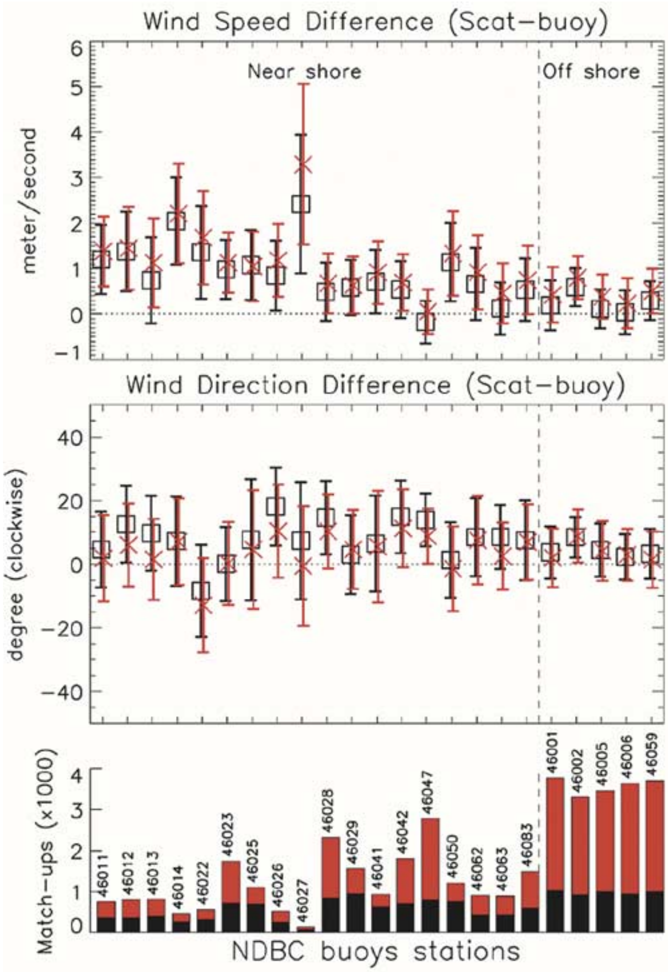

Fig. 3.(Top) Wind speed and (middle) direction residuals (scat-buoy). (Symbols) Mean average and (vertical lines) standard deviation, as well as number of pairs at each buoy location (number on top of bar indicates buoy station id), for (red) QuikSCAT data HR and (black) LR.

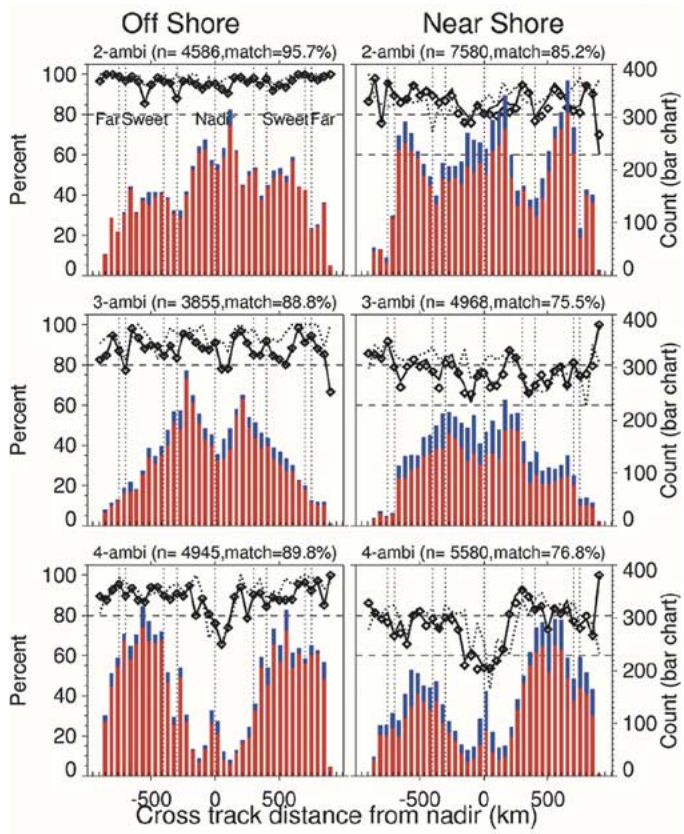

Fig. 4. Ambiguity removal skill is assessed in cases of 2-, 3-, and 4-ambiguious solutions from top to bottom (left) in the open ocean and (right) near shore, as a function of cross-track distance. The tops of the bars represent the total number of pairs in bins of 50 km, and red bars indicate counts of selected wind vector closest to the buoy measurement. Line plots show the ambiguity removal skill for (symbol) HR, (off 25 km) (solid line) HR, and (dotted line) LR. Vertical lines depict zones boundaries.

77.7%. It is interesting to note that although excluding coastal data caused the number of collocated pairs reduced by more than 15%, the skill (solid line) remained very close to those with coastal data included (symbols), in Fig. 4.

On the other hand, light wind dramatically affects the performance of the ambiguity removal algorithm. After excluding records with buoy wind speed less than 6 m/s, the integrated ambiguity removal skill for HR increase to 98.1%, 93.1%, and 92.9% for 2-, 3-, and 4-ambiguities near shore, and 99.2%, 96.2%, and 96.7% offshore. Similar ratios for LR data are 98.9%, 95.5%, and 92.3% near shore, and 99.9%, 99.0%, and 97.8% offshore.

C. DIR Improvement

As seen in Fig. 4, the worst performance area of the ambiguity removal algorithm is around the satellite nadir, where the ambiguity removal skill is less than 60% at near-shore locations and 80% offshore. DIR is developed to alleviate the problem in the swath area where poor viewing geometry leads to greater random error in wind direction [10]. Using scatterometer data with DIR modification (LRD, HRD), a set of statistical comparisons similar to that of Section III-A were performed, and the results are summarized in Table II. As expected, improvement from DIR modification is most obvious in direction retrieval, with RMSD in direction reduced by 1° and 4° in LRD and HRD, respectively. After removing light wind, the RMSD reductions are even larger. No significant improvements were found in wind speed estimation after DIR modification.

To identify areas where DIR modification becomes necessary, collocated records were further divided into three zones, according to the cross-track distance of scatterometer measurements: nadir zone (300 km off the nadir track), sweet zone (400–700 km), and far zone (750–900 km). Presented in Fig. 5, for each zone, are the cumulative probability $P(x)$, defined as the percentage of collocated records with the absolute directional differences between scatterometer and buoy measurements less than or equal to x. It is observed that the cumulative probability curves for LR (red) stay on top in all plots, representing the best performance among all scatterometer products in all zones, at both offshore and near-shore locations. Curves for HR (black) stay lowest, showing the degradation in the high-resolution product. Blue lines in each plot depicts $P(x)$ derived from HRD, representing directional improvement in all zones, with greatest improvement in nadir zone and far

TABLE II
STATISTICAL COMPARISON BETWEEN QSCAT DATA WITH DIR MODIFICATION (LRD, HRD) AND NDBC BUOY WIND MEASUREMENT

	Off Shore Buoy Locations				Near Shore Buoy Locations			
	Number of data	Bias (Scat-buoy)	RMSD (Scat-buoy)	Correlation Coefficient	Number of data	Bias (Scat-buoy)	RMSD (Scat-buoy)	Correlation Coefficient
LRD								
Speed (m/s)								
Buoy wind speed								
>= 0 m/s	4641	0.24	0.92	0.95	8419	0.70	1.50	0.88
>= 3 m/s	4185	0.22	0.88	0.94	6669	0.49	1.38	0.87
>= 6 m/s	2757	0.21	0.89	0.90	3824	0.27	1.35	0.83
Direction (deg.)								
Buoy wind speed								
>= 0 m/s	4641	4.36	15.43	0.98	8370	7.78	25.76	0.90
>= 3 m/s	4185	4.85	11.80	0.99	6669	8.99	18.94	0.93
>= 6 m/s	2757	4.76	9.15	0.99	3824	11.97	12.62	0.96
HRD								
Speed (m/s)								
Buoy wind speed								
>= 0 m/s	16704	0.44	1.04	0.93	21667	0.96	1.76	0.85
>= 3 m/s	15280	0.40	1.02	0.93	17344	0.70	1.61	0.84
>= 6 m/s	10237	0.42	1.07	0.88	10301	0.51	1.57	0.80
Direction (deg.)								
Buoy wind speed								
>= 0 m/s	16704	3.72	17.73	0.98	21667	4.78	27.39	0.87
>= 3 m/s	15280	4.65	14.28	0.98	17344	5.77	21.22	0.91
>= 6 m/s	10237	4.95	10.38	0.99	10301	8.47	14.52	0.94
HRD (off25km)								
Speed (m/s)								
Buoy wind speed								
>= 0 m/s					17931	0.80	1.53	0.88
>= 3 m/s					14554	0.61	1.47	0.87
>= 6 m/s					8663	0.47	1.49	0.82
Direction (deg.)								
Buoy wind speed								
>= 0 m/s					17931	5.59	25.94	0.88
>= 3 m/s					14554	6.45	19.81	0.92
>= 6 m/s					8663	9.08	12.89	0.95

zone, where the cumulative probability curves been pushed amazingly to very close to that of LR. At offshore locations, in the far zone where only out-beam backscatter is available, the percentage of scatterometer measurements with 20° or less directional differences raised from 73% in HR to 86% in HRD, almost the same as LR. In the nadir zone, where suboptimal viewing geometry dominates, the percentage of collocated records with scatterometer–buoy directional difference changes from 60% in HR to 80% in HRD, even higher than 75% from LR. At near-shore locations, although overall performance is much worse than offshore, DIR still demonstrated significant improvements in wind direction retrieval. For example, the cumulative percentage of 20° or less directional error is increased from 55% to 67% in the far zone, 57% to 65% in the sweet zone, and 43% to 53% in the nadir zone. Similar analysis for wind speed (not shown) does not reveal significant DIR improvement on HR. One caveat is while DIR greatly reduces intrinsic noises and improves the wind direction retrieval for the high-resolution fields, it could also smooth out some small-scale signals, although in a minimalist fashion.

D. Analysis on Directional Residual

The directional residuals were further analyzed in each subgeometric zones. Collocated records in each subset were binned in terms of buoy wind speed, with bin size of 1 m/s. Plotted in Fig. 6 are, for each zone, far, sweet, and nadir (from top to bottom), the RMSD as a function of lowest wind speed included in the statistics. Largest wind speed included in the statistics is 25 m/s, but all plots were truncated at speed of 15 m/s, because there were not enough cases with high wind speed to draw a statistically significant conclusion. A common feature in all plots is the high-directional RMSD at light wind (less than ~3 m/s), with peaks between 50° and 60° near shore. Directional RMSD dramatically drops from its peak when speed lower bound increases to around 5–7 m/s.

At offshore locations, as shown in Fig. 6(a)–(c), the directional RMSD for the standard products LR and LRD mostly stays below 20° for wind speed between 3 and 12 m/s. Only in the nadir zone does DIR show substantial improvement in directional RMSD. For the high-resolution wind, however, DIR demonstrates its significant and necessary improvement at all speed range, especially in the far and nadir zones. With results from DIR, the lower speed bounds to satisfy the accuracy requirement of 20° RMSE were reduced to less than 3 m/s in far and sweet zones and to 4 m/s in the nadir zone. In the speed range from 3–15 m/s, DIR realized 5° to 10° reduction in the RMSE in all three zones. Particularly in the nadir zone, DIR becomes so crucial for producing valid data, as seen in Fig. 6(c), where the standard algorithm was unable to bring the directional RMSD down no matter how to adjust the lower speed bound.

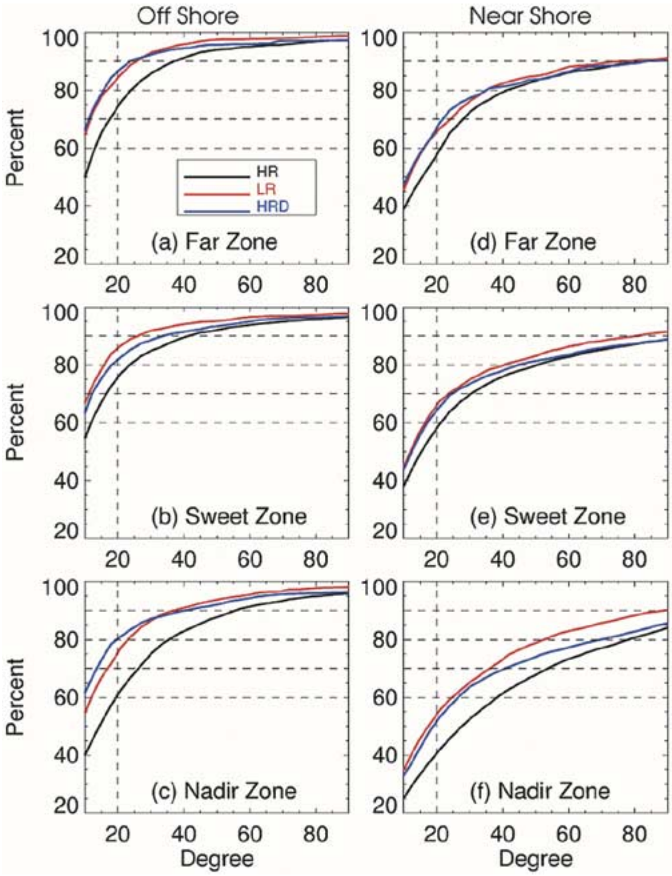

Fig. 5. Cumulative probability of directional difference (left) offshore and (right) near shore between NDBC buoys and scatterometer wind (black) HR, (red) LR, and (blue) HRD. Results are divided into three cross-track zones: (top) far (750–900 km), (middle) sweet (400–700 km), and (bottom) nadir (0–300 km).

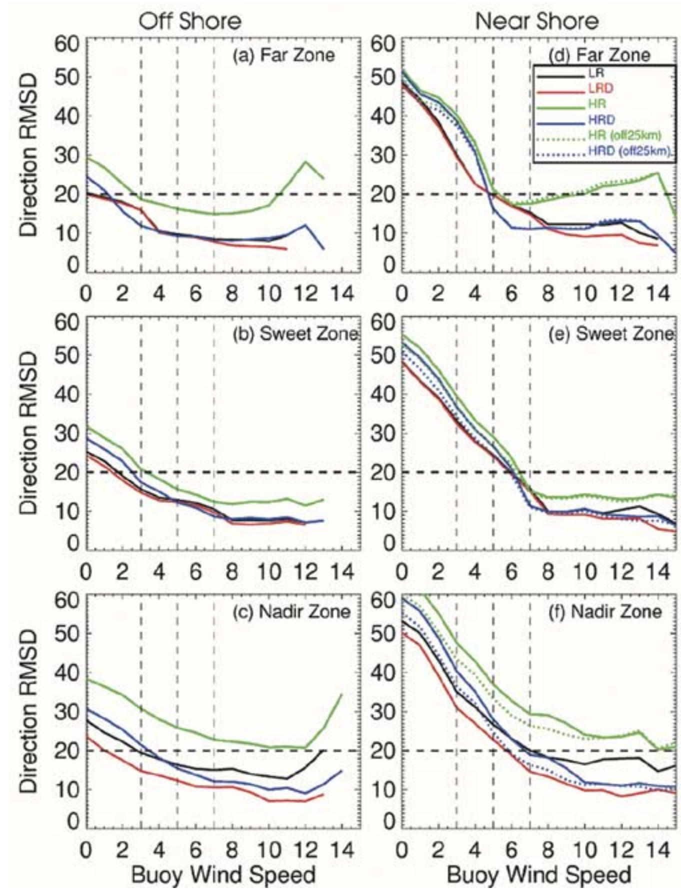

Fig. 6. Speed dependence of directional RMS error as a function of the lowest wind speed included in the statistics. Results are divided into three zones: far, sweet, and nadir (from top to bottom) for scatterometer wind (black) LR, (red) LRD, (green) HR, (blue) HRD, and dotted lines for results without data in 25-km coastal zone from the shore line: (green) HR (off 25 km) and (blue) HRD (off 25 km).

Results at near-shore locations demonstrated difficulties in the coastal region. As shown in Fig. 6(d)–(f), all scatterometer products present much higher directional errors than the offshore case. In the far zone, DIR improves directional estimation so that beyond 5 m/s, we obtained satisfactory RMSD below 20°. The nadir zone is proved again to be the most difficult area, not only for the high-resolution data. Similar to the offshore results, the directional error stays high in the nadir zone across all speed ranges without DIR modification in the high-resolution product. Excluding data in the coastal zone did bring the RMSD down slightly, but not enough to justify throwing away data in the area completely.

IV. CONCLUSION

With range-compressed σ_o, a high-resolution (12.5 km) vector wind dataset was produced in coastal ocean using the same GMF and ambiguity removal algorithm as that used in standard QuikSCAT data product. Degradation caused by noisy "slices" data and land contamination is quantified, in comparison with neutral wind at 10 m measured by NDBC buoys from different perspectives. The accuracy of the high-resolution vector wind is satisfactory in open oceans, as revealed by the analysis comparing with offshore buoys. The DIR algorithm demonstrates, in all geometric zones (far, sweet, and nadir) and a wide range of geophysical conditions (as represented by wind speed), improvements in the high-resolution wind retrieval, especially in the directional estimate. Higher RMSDs were observed near shore, from both standard products and high-resolution products. Experimental relaxation of the land contamination criteria reveals that QuikSCAT wind retrieved from "slices" that partially touches land could be useful in medium to high wind strength. Better understanding of the air–sea interaction processes in the coastal region as compared with open ocean may be needed to improve coastal wind retrieval from the scatterometer.

ACKNOWLEDGMENT

The authors thank the three anonymous reviewers for their helpful suggestions.

REFERENCES

[1] N. H. Ebuchi, H. C. Graber, and M. J. Caruso, "Evaluation of wind vectors observed by QuikSCAT/SeaWinds using ocean buoy data," *J. Atmos. Oceanic Technol.*, vol. 19, pp. 2049–2062, 2002.

[2] M. H. Freilich and R. S. Dunbar, "The accuracy of the NSCAT 1 vector winds: Comparison with national data buoy center buoys," *J. Geophys. Res.*, vol. 104, pp. 11 231–11 246, 1999.

[3] M. H. Pickett, W. Tang, L. K. Rosenfeld, and C. H. Wash, "QuikSCAT satellite comparisons with near-shore buoy wind data off the US West Coast," *J. Atmos. Oceanic Technol.*, vol. 20, pp. 1869–1879, 2003.
[4] W. T. Liu, "Progress in scatterometer application," *J. Oceanogr.*, vol. 58, pp. 121–136, 2002.
[5] JPL. (2001) QuikSCAT science data product user's manual, version 2.1. JPL Pub D18035. JPL, Pasadena, CA. [Online]. Available: http://podaac.jpl.nasa.gov/quikscat/qscat_doc.html.
[6] M. W. Spencer, C. Wu, and D. G. Long, "Improved resolution backscatter measurements with the SeaWinds pencil-beam scatterometer," *IEEE Trans. Geosci. Remote Sensing*, vol. 38, pp. 89–104, Jan. 2000.
[7] W. T. Liu, H. Hu, and S. Yueh, "Interplay between wind and rain observed in Hurricane Floyd," *Trans. AGU*, vol. 81, pp. 253–253, 2000.
[8] H. Hu and W. T. Liu, "QuikScat reveals the surface circulation of Catalina eddy," *Geophys. Res. Lett.*, vol. 29, no. 17, pp. 1821–1821, 2002.
[9] ——, "Oceanic thermal and biological responses in Santa Ana winds," *Geophys. Res. Lett.*, vol. 30, no. 11, pp. 1596–1596, 2003.
[10] D. G. Long, J. B. Luke, and W. Plant, "Ultra high resolution wind retrieval for SeaWinds," in *Proc. IGARSS*, Toulouse, France, July 21–25, 2003.
[11] Y. Chao, Z. Li, J. C. Kindle, J. D. Paduan, and F. P. Chavez, "A high-resolution surface vector wind product for coastal oceans: Blending satellite scatterometer measurements with regional mesoscale atmospheric model simulations," *Geophys. Res. Lett.*, vol. 30, no. 1, pp. 1013–1013, 2003.
[12] A. Stoffelen, "Scatterometry," Ph.D. thesis, Univ. Utrecht, The Netherlands, 1998.
[13] M. A. Portabella and A. Stoffelen, "Characterization of residual information for SeaWinds quality control," *IEEE Trans. Geosci. Remote Sensing*, vol. 40, pp. 2747–2759, Dec. 2002.
[14] B. W. Stiles, B. D. Pollard, and R. S. Dunbar, "Directional interval retrieval with thresholded nudging: A method for improving the accuracy of QuikSCAT winds," *IEEE Trans. Geosci. Remote Sensing*, vol. 40, pp. 79–89, Jan. 2002.
[15] D. B. Gilhousen, "A field evaluation of NDBC moored buoy winds," *J. Atmos. Oceanic Technol.*, vol. 4, pp. 94–104, 1987.
[16] G. D. Hamilton, "NOAA data buoy office programs," *Bull. Amer. Meteorol. Soc.*, vol. 61, pp. 1012–1017, 1980.
[17] W. T. Liu and W. Tang, "Equivalent neutral winds," Jet Propulsion Lab., Pasadena, CA, JPL Pub. 96-17, 1996.

Wenqing Tang received the Ph.D. degree in physics from the Michigan State University, East Lansing, in 1987.

She is currently a Senior Member of technical staff at the Jet Propulsion Laboratory (JPL), Pasadena, CA. Since joining JPL in 1989, she has been working on scientific analysis of earth remote sensing data to understand the role of air–sea interaction in global climate change. She is a Principal Investigator of the Office of Global Programs, National Oceanic and Atmospheric Administration, Silver Spring, MD, since 1996, responsible for the design and implementation of the data system distributing in near real-time global ocean surface vector wind data from a series of NASA scatterometers—NSCAT, QuikSCAT, and SeaWinds. She is also working on algorithm development on retrieving geophysical parameters from multiple spaceborne instruments, e.g., scatterometer, radiometer, altimeter, and ocean color sensors.

W. Timothy Liu received the Ph.D. degree in atmospheric sciences from the University of Washington, Seattle, in 1978.

He is currently a Principal Scientist at the Jet Propulsion Laboratory (JPL), California Institute of Technology, Pasadena. He has been a Principal Investigator on studies concerning ocean–atmosphere interaction and satellite oceanography since he joined JPL in 1979. He has been the Leader of the Air–Sea Interaction and Climate Team, supervising a team of meteorologists and oceanographers in their scientific researches since 1989. He has been the Project Scientist of a series of NASA scatterometer missions—NSCAT, QuikSCAT, and SeaWinds. He became a Senior Research Scientist at JPL, which is equivalent to a Full Professor in major U.S. universities, in 1993. He has served on the editorial boards of several scientific journals.

Dr. Liu is a Fellow of the American Meteorological Society. He received the Distinguished Science Award of the Pan Oceanic Remote Sensing Award Committee in 2002. In 1996, he received an Honor Professorship at China Ocean University. He received the NASA Medal for Exceptional Scientific Achievement for his pioneering work in ocean surface heat flux in 1990 and the NASA Exceptional Achievement Medal in leading the NSCAT Science Team in air–sea interaction studies in 1998. He has served on numerous science working groups and advisory panels of NASA, including the Advisory Committee of the NASA Earth Science Division. He was a member of various working groups of the World Climate Research Program and has participated in the design and implementation of field campaigns.

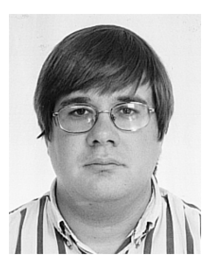

Bryan W. Stiles received the B.S. degree in electrical engineering from the University of Tennessee, Knoxville, in 1992 and the Ph.D. degree from the University of Texas, Austin, in 1997. His doctoral dissertation work proved the universal approximation capability of certain dynamic artificial neural networks.

He is currently with the Jet Propulsion Laboratory (JPL), Pasadena, CA, developing SAR, scatterometer, radiometer, and altimeter ground processing algorithms for the onboard radar on the Cassini mission to Saturn. In June 1997, he became a member of the technical staff at the JPL, where he has simulated the behavior of spaceborne scatterometers (NSCAT and SeaWinds) as well as analyzed the data returned from these instruments. He is interested in statistical techniques for determining and visualizing relationships between remote sensor data and geophysical phenomena.